Detailed statistical model analysis of observables from fusion-fission reactions

Tathagata Banerjee,* S. Nath, and Santanu Pal†
Nuclear Physics Group, Inter University Accelerator Centre, Aruna Asaf Ali Marg, Post Box 10502, New Delhi 110067, India

(Received 25 September 2018; revised manuscript received 20 January 2019; published 12 February 2019)

Background: Despite remarkable success of the statistical model (SM) in describing decay of excited compound nuclei (CN), reproduction of the observables from heavy ion-induced fusion-fission reactions is often quite challenging. Ambiguities in choosing the input parameters, lack of clarity about inclusion of various physical effects in the model, and contradictory requirements of input parameters while describing different observables from similar reactions are among the major difficulties of modeling decay of fissile CN.
Purpose: This work attempts to overcome the existing inconsistencies by inclusion of important physical effects in the model and through a systematic analysis of a large set of data over a wide range of CN mass (A_{CN}).
Method: The model includes the shell effect in the level density (LD) parameter, shell correction in the fission barrier (B_f), the effect of the orientation degree of freedom of the CN spin (K_{or}), collective enhancement of level density (CELD), and dissipation in fission. Input parameters are not tuned to reproduce observables from specific reaction(s) and the reduced dissipation coefficient (β) is treated as the only adjustable parameter. Calculated evaporation residue (ER) cross sections (σ_{ER}), fission cross sections (σ_{fiss}), and particle, i.e., neutron, proton, and α particle, multiplicities are compared with data covering $A_{CN} = 156$–248.
Results: The model produces reasonable fits to ER and fission excitation functions for all the reactions considered in this work. Pre-scission neutron multiplicities (ν_{pre}) are underestimated by the calculation beyond $A_{CN} \sim 200$. An increasingly higher value of β, in the range of 2–4 $\times 10^{21}$ s^{-1}, is required to reproduce the data with increasing A_{CN}. Proton and α-particle multiplicities, measured in coincidence with both ERs and fission fragments, are in qualitative agreement with model predictions.
Conclusions: The present work mitigates the existing inconsistencies in modeling statistical decay of the fissile CN to a large extent. Contradictory requirements of fission enhancement—obtained by scaling down the fission barrier to reproduce σ_{ER} or σ_{fiss} and fission suppression realized by introducing dissipation in the fission channel to reproduce ν_{pre}, for similar reactions—have now become redundant. There are scopes for further refinement of the model, as is evident from the mismatch between measured and calculated particle multiplicities in a few cases.

DOI: 10.1103/PhysRevC.99.024610

I. INTRODUCTION

Concepts of statistical mechanics have been applied to describe the decay of an excited compound nucleus (CN) since it was hypothesized by Bohr [1] as a mono-nucleus fully equilibrated in all degrees of freedom with no memory of its formation except the conserved quantities such as energy and angular momentum. The resulting formalism, termed generally as the statistical model (SM) of decay of the CN, has been quite successfully employed in reproducing observables from fusion reactions over the last several decades. There are, yet, certain ambiguities and inconsistencies in interpreting results from heavy ion-induced fusion-fission reactions [2,3]. We start with a few of the open questions:

(1) Simultaneous reproduction of evaporation residue (ER) cross section (σ_{ER}), fission cross section (σ_{fiss}), and pre-scission neutron, proton, and α-particle multiplicities (ν_{pre}, π_{pre}, and α_{pre}) has not been successful till date. As a consequence, it has become an accepted practice to reproduce the measured quantities by tuning the SM parameters, viz., level density parameters at ground state and saddle, a scaling factor for the fission barrier, a pre-saddle delay, and saddle-to-scission transition time [4–10]. Several combinations of those SM parameters could reproduce the data [11–13]. One naturally wonders if there is a way to reproduce data without *ad hoc* manipulation of the SM parameters.
(2) While a speeding up of fission, by means of reducing the fission barrier, was required to reproduce measured σ_{ER} [14–16], a slowing down of fission was necessary to reproduce experimental ν_{pre} [17,18]. Does this contradiction point to an inadequate modeling of CN decay?
(3) The SM fails to reproduce the particle multiplicities measured in coincidence with fission fragments (FFs) (ν_{pre}, π_{pre}, and α_{pre}) and with ERs (ν_{ER}, π_{ER} and α_{ER}), simultaneously [19]. Can this inconsistency be overcome?

*Present address: Department of Nuclear Physics, Research School of Physics and Engineering, The Australian National University, Canberra ACT 0200, Australia; he.tatha@gmail.com
†Formerly with Physics Group, Variable Energy Cyclotron Centre, 1/AF Bidhan Nagar, Kolkata 700064, India.

(4) Though disentangling pre-scission particle emissions from post-scission emissions is possible experimentally, it is fraught with difficulties in case of the particles emitted in pre-saddle and post-saddle regimes [20]. One can estimate the pre-scission dissipation coefficient from the analysis of light particle spectra and giant dipole resonance (GDR) γ-ray multiplicities [20–24]. But, to acquire a precise and reliable information about the pre-saddle dissipation coefficient, one must employ those experimental signatures which are uniquely sensitive to the pre-saddle regime only, such as σ_{ER} [25] and ER spin distribution [26]. Different combinations of pre-saddle and saddle-to-scission dissipation coefficients enabled success in interpreting particle multiplicity data [21,22,24,27]. Is it possible to determine the pre-saddle dissipation coefficient accurately?

In this article, we present a consistent SM description of observables from heavy ion-induced fusion-fission reactions with the reduced dissipation coefficient (β) as the only adjustable parameter. We shall apply the shell effect to the level density (LD) and shell correction to the fission barrier (B_f). Effects of orientation degree of freedom of CN spin (K_{or}) and collective enhancement of LD (CELD) are also included in the present model. We aim in this work to include all the effects which impact fission and various evaporation widths in order to fit a broad range of data with a minimum of adjustment of input parameters. A shorter version of the results obtained from SM calculations with the aforementioned effects has been reported earlier [2]. Fission cross sections for a few systems were also obtained using the same methodology in a previous publication [28]. Here we present results for a larger set of systems and for a wider range of experimental observables. In particular, proton and α multiplicity calculations are reported in the present work in addition to neutron multiplicity and fission/ER cross-section calculation results. Further, the neutron multiplicity and fission/ER cross-section calculations for highly fissile compound nuclei are included in the present work, thus pushing the fission model under study to the regime where almost all the compound nuclei encounter either a small or no fission barrier.

In order to compare the predictions of the present SM with data, we choose those reactions for which non-CN fission (NCNF) is predicted to be small on the basis of a systematic analysis of ER cross sections [29]. We consider here population of ^{156}Er, ^{170}Yb, ^{192}Pt, ^{197}Tl, ^{200}Pb, ^{210}Po, ^{216}Ra, ^{239}Np, and ^{248}Cf CN, each by at least two different entrance channels. The list of reactions is presented in Table I. We compare σ_{ER}, σ_{fiss}, and ν_{pre} (ν_{ER}, in a few cases) of these reactions with the predictions of the present model. We further compare π_{ER}, π_{pre}, α_{ER}, and α_{pre} of eight reactions having $A_{CN} = 158$–225 with the model predictions. Table II contains the list of these reactions.

The article is organized as follows. The various ingredients of the SM calculations and the results are presented in Sec. II followed by a discussion in Sec. III. We summarize and conclude in Sec. IV.

TABLE I. List of reactions for which measured σ_{ER}, σ_{fiss}, and ν_{pre} are compared with model predictions. Comparisons are shown in Figs. 3–6.

Reaction	CN	Ref.	Reaction	CN	Ref.
^{12}C + ^{144}Sm	^{156}Er	[30]	^{64}Ni + ^{92}Zr	^{156}Er	[30,31]
^{12}C + ^{158}Gd	^{170}Yb	[32,33]	^{16}O + ^{154}Sm	^{170}Yb	[17,32,34–36]
^{20}Ne + ^{150}Nd	^{170}Yb	[33,37–39]	^{4}He + ^{188}Os	^{192}Pt	[40–42]
^{16}O + ^{176}Yb	^{192}Pt	[42,43]	^{16}O + ^{181}Ta	^{197}Tl	[5,44–47]
^{19}F + ^{178}Hf	^{197}Tl	[47]	^{16}O + ^{184}W	^{200}Pb	[36,48–51]
^{19}F + ^{181}Ta	^{200}Pb	[17,18,52]	^{30}Si + ^{170}Er	^{200}Pb	[18,53,54]
^{1}H + ^{209}Bi	^{210}Po	[55–60]	^{4}He + ^{206}Pb	^{210}Po	[42,57,61]
^{12}C + ^{198}Pt	^{210}Po	[62–64]	^{18}O + ^{192}Os	^{210}Po	[18,52,63]
^{12}C + ^{204}Pb	^{216}Ra	[65–67]	^{19}F + ^{197}Au	^{216}Ra	[65,67]
^{30}Si + ^{186}W	^{216}Ra	[65]	^{1}H + ^{238}U	^{239}Np	[60,68–71]
^{7}Li + ^{232}Th	^{239}Np	[72,73]	^{11}B + ^{237}Np	^{248}Cf	[74–76]
^{16}O + ^{232}Th	^{248}Cf	[76–79]			

II. STATISTICAL MODEL CALCULATIONS

A. The model

In the SM calculations, the time evolution of a CN (an event) is followed over small time steps, and the fate of the CN at each time step is decided by a Monte Carlo sampling of the decay widths of various channels. The CN can follow various decay routes depending upon the relative probabilities of different decay channels. We consider fission along with emission of neutrons, protons, α particles and γ rays as the decay channels of a CN. A CN can either undergo fission with or without preceding evaporation of particles and photons or reduce to an ER. The final results for different observables are obtained as averages over a large ensemble of events. We assume the dominant fission mode to be symmetric, and the fission width is obtained from the transition-state model of fission due to Bohr and Wheeler [86]. The particle and γ decay widths are obtained from the Weisskopf formula as given in Ref. [23].

The evaporation and fission widths depend upon the spin of the CN, hence the spin distribution of CN, formed in a fusion-fission reaction, is required in SM calculations. We obtain this distribution by assuming that the whole of the incident flux in the entrance channel is absorbed to form a CN. Therefore we consider the fusion cross section to be the same as the capture cross section and obtain the spin distribution of the CN from the coupled-channels code CCFULL [87] using coupling constants and excitation energies of the low-lying

TABLE II. List of reactions for which measured σ_{ER}, proton, and α-particle multiplicities are compared with model predictions. Comparisons are shown in Figs. 7 and 8.

Reaction	CN	Ref.	Reaction	CN	Ref.
^{32}S + ^{126}Te	^{158}Er	[80]	^{19}F + ^{159}Tb	^{178}W	[81]
^{28}Si + ^{165}Ho	^{193}Tl	[8]	^{19}F + ^{181}Ta	^{200}Pb	[17,82–84]
^{16}O + ^{197}Au	^{213}Fr	[8,14,82]	^{19}F + ^{197}Au	^{216}Ra	[82]
^{16}O + ^{208}Pb	^{224}Th	[8,14,85]	^{28}Si + ^{197}Au	^{225}Np	[82]

collective states of both the projectile and the target nucleus. The CN spin distribution, thus obtained, is used as input to the SM calculation.

The fission barrier in the present calculation is obtained by including shell correction in the liquid-drop nuclear mass. The macroscopic part of the fission barrier is given by the finite-range liquid drop model (FRLDM) which was obtained earlier by fitting the systematic behavior of ground state masses and fission barriers at low angular momentum for nuclei over a wide range of masses [88]. The shell correction term δ is defined as the difference between the experimental and the liquid-drop model (LDM) masses,

$$\delta = M_{\rm exp} - M_{\rm LDM}. \tag{1}$$

The full fission barrier $B_{\rm f}(\ell)$ of a nucleus carrying angular momentum ℓ is then given as

$$B_{\rm f}(\ell) = B_{\rm f}^{\rm LDM}(\ell) - (\delta_{\rm g} - \delta_{\rm s}), \tag{2}$$

where $B_{\rm f}^{\rm LDM}(\ell)$ is the angular momentum dependent LDM fission barrier [88] and $\delta_{\rm g}$ and $\delta_{\rm s}$ are the shell correction energies for the ground-state and saddle configurations, respectively. The shell corrections at ground state and saddle are obtained following the recipe given in Ref. [89] for including deformation dependence in the shell correction energy. This yields a negligible shell correction at large deformations while the full shell correction is applied at zero deformation. A schematic representation of the shell effect on available phase space at ground state and saddle is given in Fig. 1.

The shell structure in nuclear single-particle levels also influences the nuclear level density which is used to calculate various decay widths of the compound nucleus. Ignatyuk *et al.* [90] proposed a level density parameter a which includes an intrinsic excitation energy (E^*) dependent shell effect term and is given as

$$a(E^*) = \tilde{a}\left[1 + \frac{1 - \exp\left(-\frac{E^*}{E_{\rm D}}\right)}{E^*}\delta\right]. \tag{3}$$

Here, $E_{\rm D}$ is a parameter which determines the rate at which the shell effect decreases with increase of E^*. The above form of the level density parameter used in the present work exhibits shell effects at low excitation energies and goes over to its asymptotic value at high excitation energies. The following asymptotic shape-dependent level density parameter is taken from the work of Reisdorf [91]:

$$\tilde{a} = 0.04543 r_0^3 A + 0.1355 r_0^2 A^{\frac{2}{3}} B_{\rm s} + 0.1426 r_0 A^{\frac{1}{3}} B_{\rm k}, \tag{4}$$

where A is the nuclear mass number, r_0 is the nuclear radius parameter, and $B_{\rm s}$ and $B_{\rm k}$ are respectively the surface and curvature terms of the liquid drop model. The values of r_0 and $E_{\rm D}$ are fixed by fitting the available s-wave neutron resonance spacings [91].

The nuclear level density considered so far corresponds to that of a Fermi gas with the effect of shell structure included at lower excitations. However, residual interaction in the nuclear Hamiltonian can give rise to correlation among particle-hole states resulting in collective excitations. The energy levels of these collective states are often considerably lower than the noninteracting particle-hole states from which they are

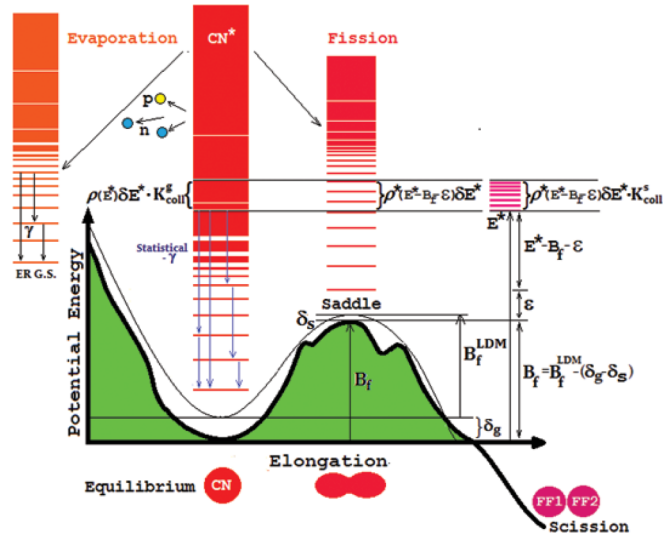

FIG. 1. Potential energy as a function of elongation. The fission barrier ($B_{\rm f}$) and the density of states [$\rho(E^*)$] change when shell corrections and CELD are taken into account, leading to modification of the Bohr-Wheeler fission width. $\rho(E^*)\delta E^*$ is the number of quantum states between energies E^* and $E^* + \delta E^*$ at the ground state (i.e., local minima with zero potential energy). The number of quantum states at the saddle point, with inclusion of shell corrections, would be $\rho(E^* - B_{\rm f} - \epsilon)\delta E^*$, where ϵ is the associated kinetic energy. With the incorporation of CELD, the same would be modified to $\rho(E^* - B_{\rm f} - \epsilon)\delta E^* \times K_{\rm coll}^{\rm s}$ and also the number of states available at the ground state would become $\rho(E^*)\delta E^* \times K_{\rm coll}^{\rm g}$. $\delta_{\rm g}$ and $\delta_{\rm s}$ are shell correction energies at the ground state and the saddle point, respectively. See text for details.

formed. Inclusion of collective states therefore enhances the level density obtained with the independent particle model at low excitation energies. The collective enhancement of level density (CELD) was considered earlier by Bjornholm, Bohr, and Mottelson [92] where the collective levels were generated by adding additional degrees of freedom to those of the Fermi gas. They further argued that the effect of double counting of states can be neglected since the excitation energy of the particle-hole states which are involved in the collective states are so high that there are many more states at these energies in the Fermi gas which do not contribute to the collective states. The total level density $\rho(E^*)$ can therefore be written as [92]

$$\rho(E^*) = K_{\rm coll}(E^*)\rho_{\rm intr}(E^*), \tag{5}$$

where $\rho_{\rm intr}(E^*)$ is the intrinsic level density and $K_{\rm coll}$ is the collective enhancement factor. The rotational and vibrational enhancement factors are obtained as

$$K_{\rm rot} = \frac{\tau_\perp T}{\hbar^2}, \tag{6a}$$

$$K_{\rm vib} = e^{0.055 \times A^{\frac{2}{3}} \times T^{\frac{4}{3}}}, \tag{6b}$$

where T is the nuclear temperature and $\tau_\perp$ is the rigid body moment of inertia perpendicular to the symmetry axis [93]. A

smooth transition from $K_{\rm vib}$ to $K_{\rm rot}$ with increasing quadrupole deformation $|\beta_2|$, was obtained by Zagrebaev *et al.* [94],

$$K_{\rm coll}(|\beta_2|) = [K_{\rm rot}\varphi(|\beta_2|) + K_{\rm vib}(1-\varphi(|\beta_2|))]\, f(E^*), \quad (7a)$$

using a function $\varphi(|\beta_2|)$ given as

$$\varphi(|\beta_2|) = \left[1+\exp\left(\frac{\beta_2^0 - |\beta_2|}{\Delta\beta_2}\right)\right]^{-1}, \quad (7b)$$

and the damping of collective effects with increasing excitation is accounted for by the functional form [95]

$$f(E^*) = \left[1+\exp\left(\frac{E^* - E_{\rm cr}}{\Delta E}\right)\right]^{-1}. \quad (7c)$$

The values of $\beta_2^0 = 0.15$ and $\Delta\beta_2 = 0.04$ are taken from Ref. [96]. The values of $E_{\rm cr}$ and ΔE are taken as 40 and 10 MeV, respectively, which were obtained by fitting yields from projectile fragmentation experiments [95]. The effect of damping of CELD with increasing excitation energy has also been experimentally observed in evaporation spectra of neutrons and high energy photons [97,98].

From the transition-state theory of Bohr and Wheeler [86], the fission width for a nucleus with total excitation energy E^* and angular momentum ℓ is given as

$$\Gamma_{\rm f}^{\rm BW}(E^*,\ell,K=0) = \frac{1}{2\pi\,\rho_{\rm g}(E^*)}\int_0^{E^*-B_{\rm f}(\ell)} \rho_{\rm s}(E^*-B_{\rm f}(\ell)-\epsilon)d\epsilon, \quad (8)$$

where

$$E^* = E - E_{\rm rot}(\ell) - E_{\rm pair} \quad (9)$$

is the intrinsic or thermal part of E and $E_{\rm rot}(\ell)$ and $E_{\rm pair}$ are the rotational and pairing energies, respectively. $\rho_{\rm g}$ and $\rho_{\rm s}$ denote the level densities at the ground state and the saddle configurations, respectively, as given by Eq. (5). $B_{\rm f}(\ell)$ is the angular momentum dependent fission barrier, defined by Eq. (2).

The above fission width is obtained under the assumption that the orientation of the angular momentum remains perpendicular to both the reaction plane and the symmetry axis throughout the course of the reaction. Therefore the angular momentum component along the symmetry axis (K) is set equal to zero in the above equation. However, the intrinsic nuclear motion can perturb the CN angular momentum and cause to change its orientation from the initial direction perpendicular to the symmetry axis [13], as schematically illustrated in Fig. 2. Therefore, K can assume nonzero values during the fission process. Since the moment of inertia parallel to the symmetry axis is smaller than that in the perpendicular direction, the rotational energy at the saddle, and consequently the fission barrier, is higher for $K \neq 0$ states than that for $K = 0$. If a fast equilibration of the K degree of freedom is assumed, the fission width can be obtained

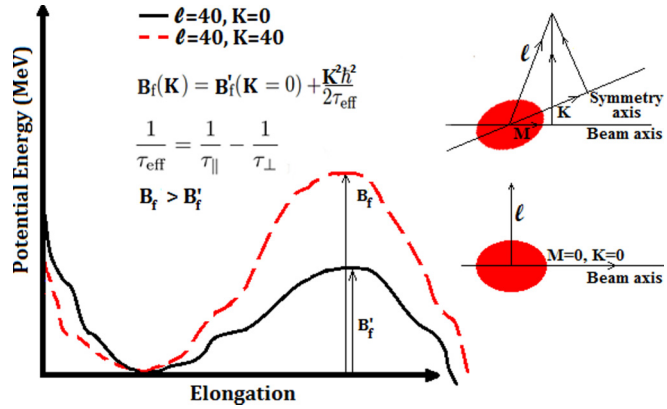

FIG. 2. The effect of K degree of freedom ($K_{\rm or}$) on $B_{\rm f}$. The increased value of $B_{\rm f}$ would reduce the fission width. See text for details.

as [99]

$$\Gamma_{\rm f}^{\rm BW}(E^*,\ell,K) = \Gamma_{\rm f}^{\rm BW}(E^*,\ell,K=0)\frac{(K_0\sqrt{2\pi})}{2\ell+1}\,{\rm erf}\left(\frac{\ell+1/2}{K_0\sqrt{2}}\right) \quad (10)$$

with

$$K_0^2 = \frac{\tau_{\rm eff}}{\hbar^2}T_{\rm sad}, \quad (11a)$$

$$\frac{1}{\tau_{\rm eff}} = \frac{1}{\tau_\parallel} - \frac{1}{\tau_\perp}, \quad (11b)$$

where $T_{\rm sad}$ is the temperature at saddle and $\tau_{\rm eff}$ is the effective moment of inertia. $\tau_\perp$ and $\tau_\parallel$ are the moments of inertia at saddle of the nucleus perpendicular to and about the nuclear symmetry axis. The above definition of K_0^2 from the transition state model of fission explains the fission fragment angular distribution satisfactorily. erf(x) denotes the error function.

Numerous studies in the past have established that a slowing down of the fission process, in comparison to that given by the Bohr-Wheeler fission width is required in order to reproduce measured $\nu_{\rm pre}$ (see, e.g., [13]). In such cases, the available phase space at saddle (as in Bohr-Wheeler theory) alone does not determine the fission rate, but the dynamical evolution of the nuclear shape from ground state to the scission point past the saddle point is to be taken into account. The process closely resembles to the dynamics of a Brownian particle in a heat bath placed in a potential pocket. The escape rate across the potential barrier or the fission rate was obtained by Kramers [100] many years ago. A reduction in fission width is obtained from the dissipative stochastic dynamical model of fission developed by Kramers where the fission width is given as [100]

$$\Gamma_{\rm f}^{\rm Kram}(E^*,\ell,K) = \Gamma_{\rm f}^{\rm BW}(E^*,\ell,K)\left\{\sqrt{1+\left(\frac{\beta}{2\omega_s}\right)^2} - \frac{\beta}{2\omega_s}\right\}, \quad (12)$$

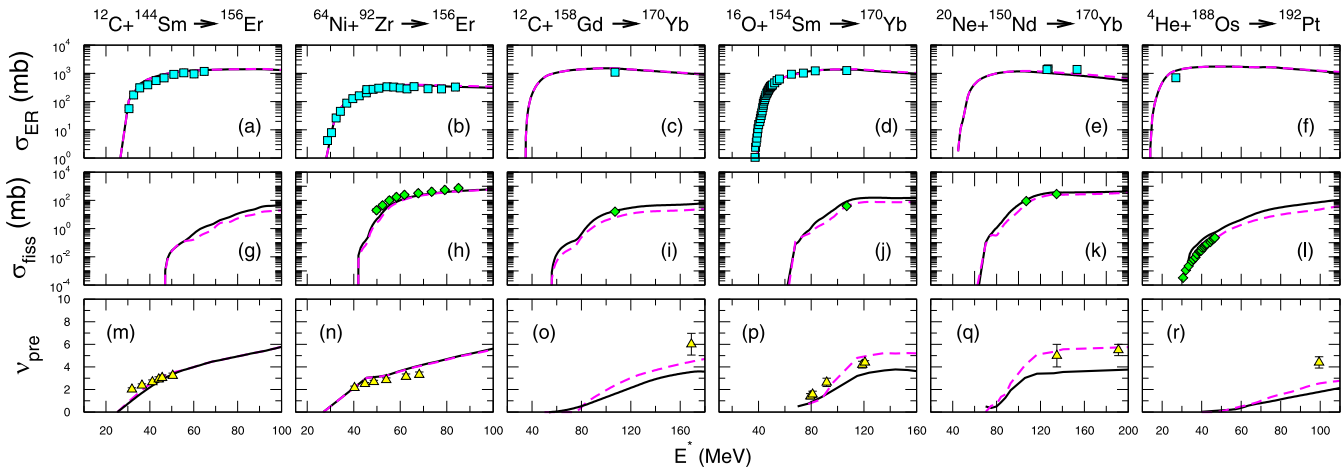

FIG. 3. Comparison of measured σ_{ER}, σ_{fiss}, and ν_{pre} with SM predictions for the reaction $^{12}C + ^{144}Sm$ [30], $^{64}Ni + ^{92}Zr$ [30,31], $^{12}C + ^{158}Gd$ [32,33], $^{16}O + ^{154}Sm$ [17,32,34–36], $^{20}Ne + ^{150}Nd$ [33,37–39], and $^{4}He + ^{188}Os$ [40–42]. Neutron multiplicities of $^{12}C + ^{144}Sm$ and $^{64}Ni + ^{92}Zr$ were measured and calculated in coincidence with ER. Continuous (black) lines indicate the SM predictions including shell correction both in B_f and LD, CELD and K-orientation effects. Dashed (magenta) lines show results with all the aforementioned effects and $\beta = 2 \times 10^{21}$ s^{-1}.

where β is the reduced dissipation coefficient (ratio of dissipation coefficient to inertia) and ω_s is the local frequency of a harmonic oscillator potential which approximates the nuclear potential at the saddle configuration and depends on the spin of the CN [101]. $\Gamma_f^{BW}(E^*, \ell, K)$ is the Bohr-Wheeler fission width obtained after incorporating shell corrected level densities, CELD, and the K-orientation effect. Though nuclear dissipation has been a subject of considerable amount of theoretical research, its precise nature and magnitude are yet to be established [102–104]. On the other hand, extraction of dissipation coefficient from fitting of experimental data is model dependent to some extent. We, therefore, choose to treat β as an adjustable parameter to fit experimental data in the present work.

In a stochastic dynamical model of fission, a certain time interval elapses before the fission rate reaches its stationary value as given by Eq. (12) [105]. A parametrized form of time-dependent fission width is given as [106]

$$\Gamma_f^{Kram}(E^*, \ell, K, t) = \Gamma_f^{Kram}(E^*, \ell, K)\left\{1 - e^{-\frac{2.3t}{\tau_f}}\right\} \quad (13)$$

where

$$\tau_f = \frac{\beta}{2\omega_g^2} \ln\left(\frac{10B_f(\ell)}{T}\right) \quad (14)$$

is the transient time period while the potential near the ground state is approximated by a harmonic oscillator potential of frequency ω_g.

The fission widths given by Bohr and Wheeler or Kramers are obtained under the assumption that fission occurs when the CN shape crosses the saddle point deformation. The number of neutrons evaporated prior to fission obtained in the SM calculation therefore refers to those neutrons emitted till the CN reaches the saddle point deformation. The experimentally determined ν_{pre}, however, includes all neutrons emitted till the CN splits into two FFs. Thus neutrons emitted during saddle-to-scission transition of the CN are also included in experimental ν_{pre}. The saddle-to-scission neutron multiplicity is obtained in the present SM calculation by using the saddle-to-scission time interval, which is given as [107]

$$\tau_{ss} = \tau_{ss}^0 \left\{\sqrt{1 + \left(\frac{\beta}{2\omega_s}\right)^2} + \frac{\beta}{2\omega_s}\right\}, \quad (15)$$

where τ_{ss}^0 is the saddle-to-scission transit time without any dissipation [105,107].

The above features are incorporated in an SM code VECSTAT [2]. Excitation functions of fission and ER and multiplicities of evaporated light particles are calculated for a number of fusion-fission reactions.

B. Results

The calculated σ_{ER}, σ_{fiss}, and ν_{pre} (ν_{ER}, in a few cases) for several fusion-fission reactions are shown in Figs. 3–6 in increasing order of A_{CN}. The available experimental values are also shown in the plots. The CN formed in the above reactions range from that of a low fissility ($\chi_{CN} = 0.600$ for ^{156}Er) to a high one ($\chi_{CN} = 0.826$ for ^{248}Cf). Consequently, the dominating reaction products also change from ERs to FFs across the systems considered here.

Two sets of SM results are displayed in Figs. 3–6, where one set includes shell correction applied to both $B_f(\ell)$ and level density and also CELD and K-orientation effects but without any dissipation while the other set includes dissipation in addition to the above-mentioned effects. It is observed that, in general, SM results without dissipation overestimate σ_{fiss} but underestimate σ_{ER} and ν_{pre}. A value for β is next chosen to fit the experimental data. Since the effect of dissipation in fission width in Eq. (12) is obtained by considering fission dynamics in the pre-saddle region [100], β in Eq. (12) also corresponds to the reduced dissipation coefficient in the same region. Further, the most unambiguous signature of CN formation and subsequent decay is the ER cross section.

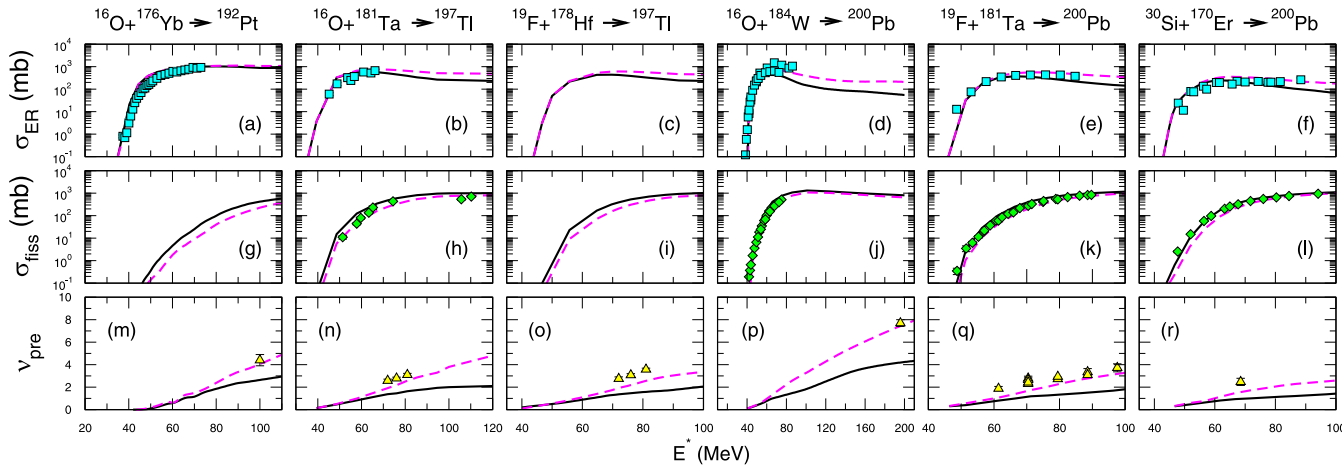

FIG. 4. Comparison of measured σ_{ER}, σ_{fiss}, and ν_{pre} with SM predictions for the reactions $^{16}O + ^{176}Yb$ [42,43], $^{16}O + ^{181}Ta$ [5,44–47], $^{19}F + ^{178}Hf$ [47], $^{16}O + ^{184}W$ [36,48–51], $^{19}F + ^{181}Ta$ [17,18,52], and $^{30}Si + ^{170}Er$ [18,53,54]. Continuous (black) lines indicate the SM predictions including shell correction both in B_f and LD, CELD and K-orientation effects. Dashed (magenta) lines show results with all the aforementioned effects and $\beta = 2 \times 10^{21}$ s^{-1}.

We therefore adjust the strength of β in order to fit the ER excitation function. It may, however, be mentioned that β in Eq. (15) represents the reduced dissipation coefficient in the saddle-to-scission region. Though the strength of β in the pre-saddle and the post-saddle regimes need not be the same, we use the same value for both in the present work.

It is observed that $\beta = 2 \times 10^{21}$ s^{-1} gives reasonable fit to ER and also to fission excitation functions up to $A_{CN} \sim 200$, though ν_{pre} are underpredicted in certain cases (Figs. 3 and 4). A higher value of $\beta = 3 \times 10^{21}$s^{-1} is found to be necessary for CN between ^{210}Po and ^{216}Ra (Figs. 5 and 6) to fit the ER excitation functions. Here too, the fission excitation functions are well reproduced but β is found to be inadequate for ν_{pre}. For highly fissile CN, i.e., ^{239}Np and ^{248}Cf, formed in light projectile-induced reactions, the SM predictions for σ_{ER} are very small and no ER data are available (Fig. 6). Since the calculated fission excitation functions are insensitive to the strength of β, the same is obtained by fitting the ν_{pre} for the above two CN. Good fits to ν_{pre} excitation functions are obtained with $\beta = 4 \times 10^{21}$ s^{-1}.

It may be noted here that β plays two roles in the present calculation: one is to impact the pre-saddle multiplicity through Eqs. (12) and (13), and the other is to control the saddle-to-scission transition time and hence multiplicity through Eq. (15). For low fissility compound nuclei, the majority of particle evaporation takes place in the pre-saddle region, and therefore β obtained for such systems corresponds to dissipation coefficient for compact shapes of the compound nuclei. On the other hand, almost all the particles are evaporated during the saddle-to-scission transition for highly fissile compound nuclei such as Np and Cf. Dissipation coefficients at large deformations of nuclear shape are thus obtained from

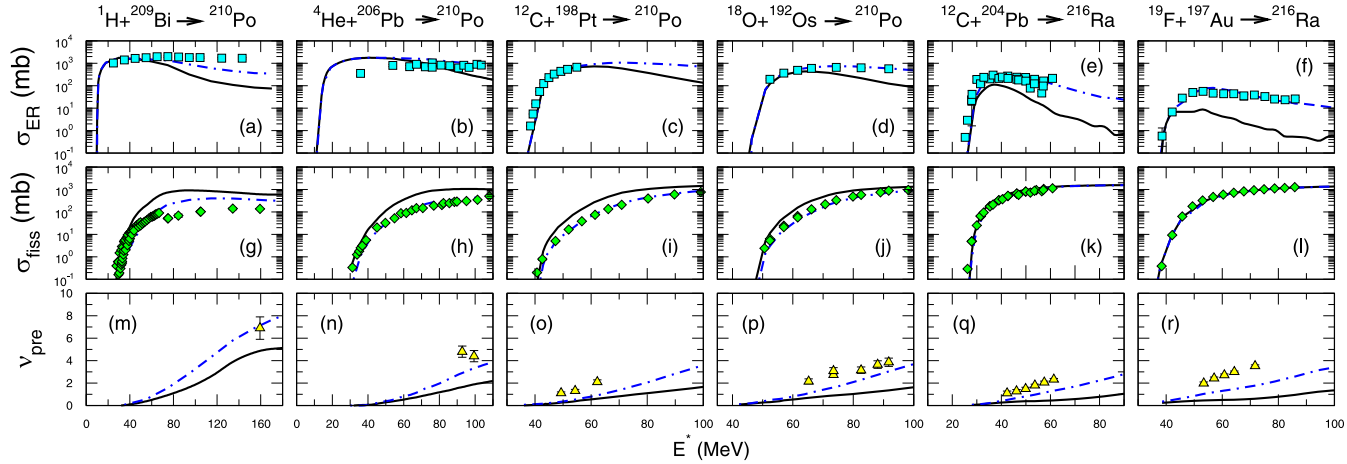

FIG. 5. Comparison of measured σ_{ER}, σ_{fiss}, and ν_{pre} with SM predictions for the reactions $^{1}H + ^{209}Bi$ [55–60], $^{4}He + ^{206}Pb$ [42,57,61], $^{12}C + ^{198}Pt$ [62–64], $^{18}O + ^{192}Os$ [18,52,63], $^{12}C + ^{204}Pb$ [65–67], and $^{19}F + ^{197}Au$ [65,67]. Continuous (black) lines indicate the SM predictions including shell correction both in B_f and LD, CELD and K-orientation effects. Dash-dotted (blue) lines show results with all the aforementioned effects and $\beta = 3 \times 10^{21}$ s^{-1}.

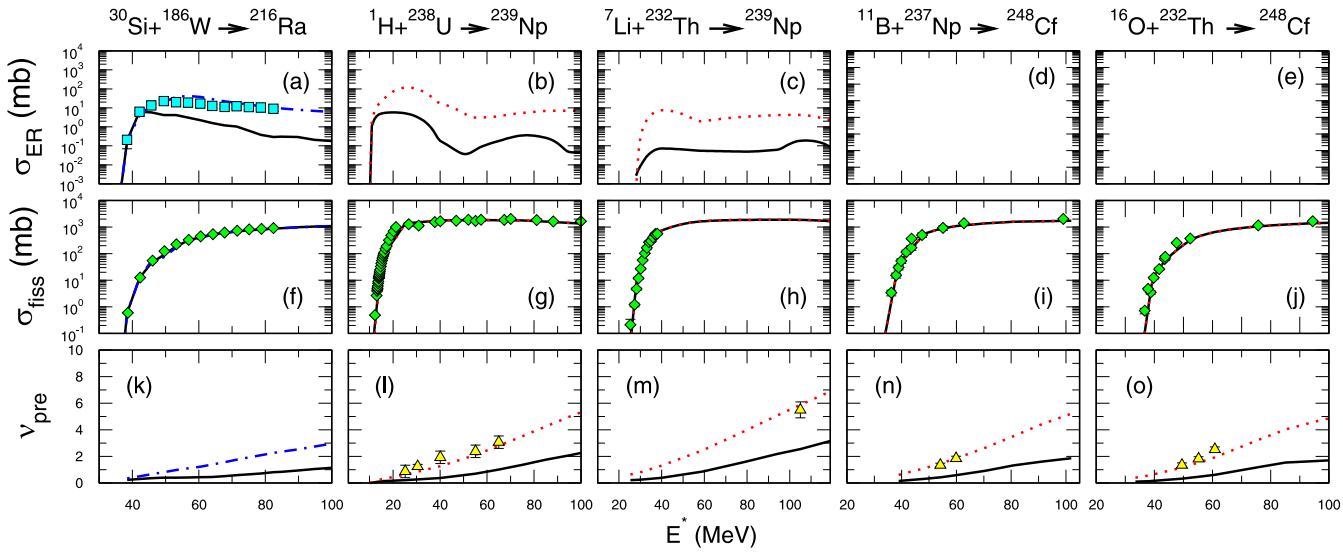

FIG. 6. Comparison of measured σ_{ER}, σ_{fiss}, and ν_{pre} with SM predictions for the reactions $^{30}Si + ^{186}W$ [65], $^{1}H + ^{238}U$ [60,68–71], $^{7}Li + ^{232}Th$ [72,73], $^{11}B + ^{237}Np$ [74–76], and $^{16}O + ^{232}Th$ [76–79]. Continuous (black) lines indicate the SM predictions including shell correction both in B_f and LD, CELD and K-orientation effects. Dash-dotted (blue) and dotted (red) lines show results with all the aforementioned effects and $\beta = 3 \times 10^{21}$ s^{-1} and $\beta = 4 \times 10^{21}$ s^{-1}, respectvely.

analysis of experimental data of highly fissile systems. In the present work, we find $\beta = 2 \times 10^{21}$ s^{-1} for light CN (Figs. 3 and 4) while 4×10^{21} s^{-1} for Np and Cf (Fig. 6). For compound nuclei with intermediate masses, 3×10^{21} s^{-1} is found to be more appropriate (Fig. 5).

We therefore find the dissipation strength increases with deformation of a nucleus. Such a shape-dependent dissipation strength is also predicted from consideration of chaos in the single-particle motion in the "chaos-weighted wall formula" (CWWF) [108]. The CWWF dissipation strength for compact shapes is about (0–3) $\times 10^{21}$ s^{-1}, while it increases to about 6×10^{21} s^{-1} for large deformation. Interestingly, β values obtained in the present analysis are also close to the strength of CWWF. It may further be pointed out that several earlier works [22,23] also used empirical shape-dependent dissipation in statistical model analysis of experimental data. However, the earlier studies did not include all the effects which impact different decay channels considered in the present work and noninclusion of one or the other effect can affect the fitted value of dissipation strength. Since all such effects are included in the present work, we expect the fitted values of β to represent the true strength of nuclear dissipation.

We next consider charged particle multiplicities in coincidence with either ERs or FFs in fusion-fission reactions. SM predictions for proton and α-particle multiplicities in the ER channels for a number of reactions are shown in Fig. 7 along with the experimental data. The ER excitation functions are also given in this figure. The dissipation strength in SM calculation is adjusted to fit the ER excitation functions, and no other parameter is tuned to fit the charged particle multiplicities. The fission probability of CN has no direct effect on particle multiplicities from ERs except influencing the ER angular momentum distribution and, consequently, the excitation energy available for evaporation. We therefore find that the multiplicity distributions obtained with or without dissipation are very close to each other for the systems $^{32}S + ^{126}Te$, $^{28}Si + ^{165}Ho$, and $^{19}F + ^{181}Ta$ since the ER excitation functions of the respective systems obtained with or without dissipation are also close. On the other hand, charged particle multiplicities for the systems $^{16}O + ^{197}Au$ and $^{16}O + ^{208}Pb$ are significantly reduced and σ_{ER} are substantially increased when dissipation is included in the SM calculations. This is a consequence of lowering of the average excitation energy of the ERs since they carry larger angular momentum in SM calculations with dissipation. We further observe that SM predictions match experimental data reasonably well for both proton and α-particle multiplicities from the reactions $^{32}S + ^{126}Te$, $^{28}Si + ^{165}Ho$, and $^{19}F + ^{181}Ta$. However, while close agreement with experimental data is observed for proton multiplicity, the α multiplicity is underestimated to some extent for the systems $^{16}O + ^{197}Au$ and $^{16}O + ^{208}Pb$ when dissipation is included in SM calculation. It is also found in Fig. 7 that the SM prediction with $\beta = 3 \times 10^{21}$ s^{-1} overestimates σ_{ER} at lower excitation energies for the system $^{16}O + ^{208}Pb$ though it fits the ER excitation function at higher excitation energies. These are some of the issues which require further investigation in future works.

Figure 8 shows the pre-scission proton and α-particle multiplicities for a number of systems. Both experimental values and SM predictions for charged particle multiplicities are given in this figure. SM results are obtained both with and without dissipation. The dissipation strength for a CN is taken to be the same as that used to fit the ER excitation functions in the same mass region. The SM predictions qualitatively follow the trend of experimental data. Similar to ν_{pre}, SM calculation yields larger values of multiplicities when dissipation is considered. Quantitative comparison of SM predictions with experimental data, however, does not show any definite pattern. While SM calculation with dissipation gives good fit to experimental π_{pre} for the $^{16}O + ^{197}Au$ and experimental

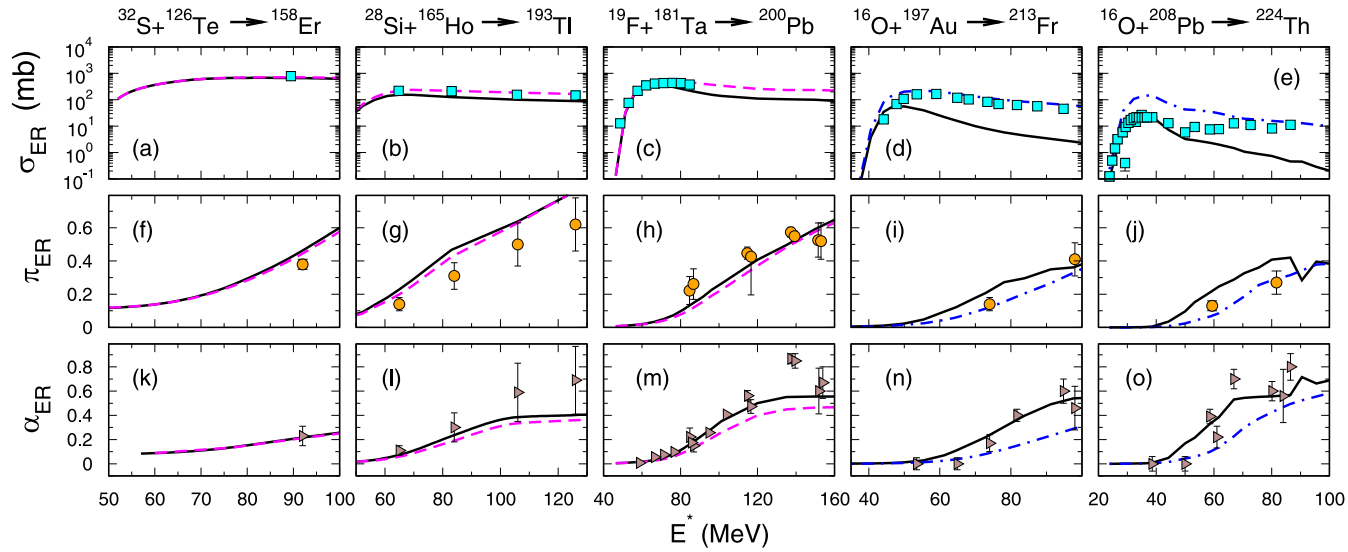

FIG. 7. Comparison of measured σ_{ER}, π_{ER}, and α_{ER} with SM predictions for the reactions $^{32}S + ^{126}Te$ [80], $^{28}Si + ^{165}Ho$ [8], $^{19}F + ^{181}Ta$ [17,83,84], $^{16}O + ^{197}Au$ [8,14], and $^{16}O + ^{208}Pb$ [8,14,85]. Continuous (black) lines indicate the SM predictions including shell correction both in B_f and LD and in CELD and K-orientation effects. Dashed (magenta) and dash-dotted (blue) lines show results with all the aforementioned effects and $\beta = 2 \times 10^{21} s^{-1}$ and $\beta = 3 \times 10^{21}$ s^{-1}, respectvely.

α_{pre} for the $^{28}Si + ^{197}Au$, SM results obtained without dissipation fit experimental π_{pre} reasonably well for $^{19}F + ^{181}Ta$, $^{19}F + ^{197}Au$, and $^{28}Si + ^{197}Au$ systems. Moreover, inclusion of dissipation though improves SM results for α_{pre} for the $^{16}O + ^{197}Au$ and $^{19}F + ^{197}Au$, they still considerably underestimate the experimental values. It may be remarked here that some part of evaporation from a CN undergoing fission can take place when it is deformed, particularly during the saddle-to-scission transition. The effect of deformation on decay widths is expected to be higher for charged particles than neutrons because of the Coulomb potential [109] which is not included in the present calculations. This may account for the deviations of SM predictions from the experimental data in certain cases. Accurate charged particles multiplicity data for more systems in both ER and fission channels will help to improve the SM further.

Thus, SM analysis of a large number of systems covering a broad range of A_{CN} and χ_{CN} show that the ER and fission excitation functions can be well reproduced when a β of strength in the range 2–4 $\times$ 10^{21} s^{-1} is included along with shell effects both in B_f and LD and in CELD and K-orientation effect. Dissipation strength of the above magnitude in fission dynamics has also been found necessary in earlier works [13,22,23]. Though SM predictions for ν_{pre} are found to be satisfactory for some systems, they tend to underestimate it for the others. The limitations of the SM in predicting pre-scission particle multiplicities are discussed in the next section.

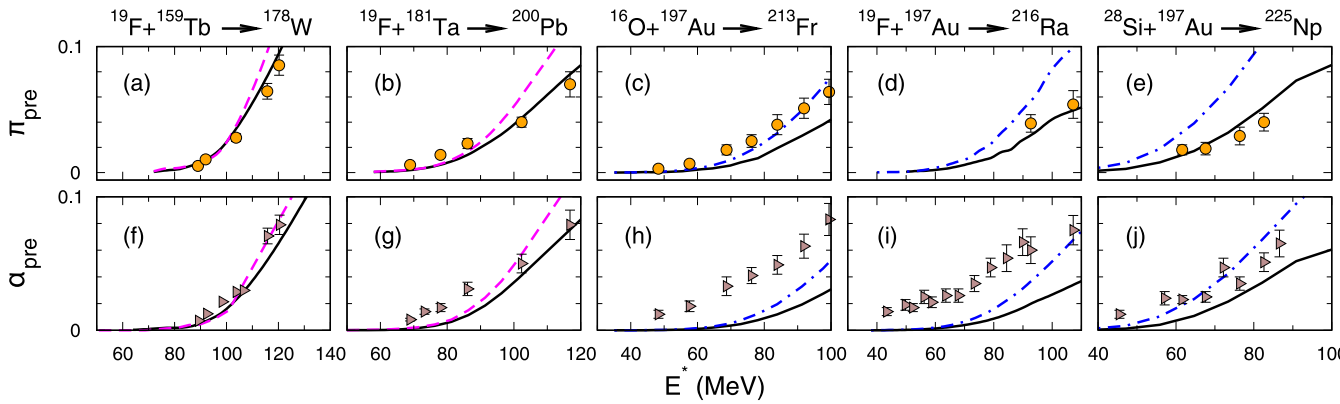

FIG. 8. Comparison of measured π_{pre} and α_{pre} with SM predictions for the reactions $^{19}F + ^{159}Tb$ [81], $^{19}F + ^{181}Ta$ [82], $^{16}O + ^{197}Au$ [82], $^{19}F + ^{197}Au$ [82], and $^{28}Si + ^{197}Au$ [82]. Continuous (black) lines indicate the SM predictions including shell correction both in B_f and LD and in CELD and K-orientation effects. Dashed (magenta) and dash-dotted (blue) lines show results with all the aforementioned effects and $\beta = 2 \times 10^{21}$ s^{-1} and $\beta = 3 \times 10^{21}$ s^{-1}, respectvely.

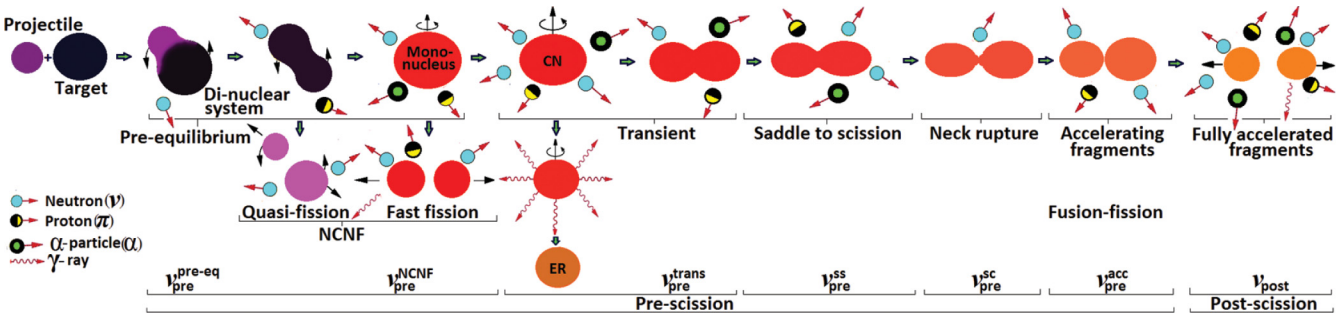

FIG. 9. Cartoon showing emission of neutrons at different stages of heavy-ion-induced fusion-fission reactions. See text for details.

III. DISCUSSION

In general, the neutron (or any other light charged particle) multiplicity in a heavy-ion-induced fusion-fission reaction comprises neutrons emitted at the following stages (see Fig. 9) of the reaction:

(1) preequilibrium composite system ($\nu_{\rm pre}^{\rm pre\text{-}eq}$),
(2) fragments originating from NCNF of the composite system ($\nu_{\rm pre}^{\rm NCNF}$),
(3) transient: ground state of CN to saddle ($\nu_{\rm pre}^{\rm trans}$),
(4) saddle to scission ($\nu_{\rm pre}^{\rm ss}$),
(5) neck rupture ($\nu_{\rm pre}^{\rm sc}$),
(6) acceleration phase of fission fragments ($\nu_{\rm pre}^{\rm acc}$),
(7) post-scission: fully accelerated fission fragments ($\nu_{\rm post}$).

The pre-scission component of the experimental neutron multiplicity ($\nu_{\rm pre}^{\rm exp}$), which is compared with SM predictions would thus be given as

$$\nu_{\rm pre}^{\rm exp} = \nu_{\rm pre}^{\rm pre\text{-}eq} + \nu_{\rm pre}^{\rm NCNF} + \nu_{\rm pre}^{\rm trans} + \nu_{\rm pre}^{\rm ss} + \nu_{\rm pre}^{\rm sc} + \nu_{\rm pre}^{\rm acc}. \quad (16)$$

The SM, however, includes only $\nu_{\rm pre}^{\rm trans}$ and $\nu_{\rm pre}^{\rm ss}$ in the calculated $\nu_{\rm pre}$ [107]. Evidently, good agreement between calculated and experimental multiplicities is expected when the contributions of other terms in Eq. (16), which are not included in the SM, are small. Further, the relative magnitudes of $\nu_{\rm pre}^{\rm trans}$ and $\nu_{\rm pre}^{\rm ss}$ depend upon the angular momentum of the CN since the fission barrier decreases with increasing angular momentum and consequently $\nu_{\rm pre}^{\rm trans}$ decreases. The saddle-to-scission interval also increases with increasing angular momentum. Thus, the relative contribution of $\nu_{\rm pre}^{\rm ss}$ increases with increasing angular momentum of the CN. The CN shape is strongly deformed in the saddle-to-scission region though its effect on particle widths has not been taken into account in the present calculation. Further, $\nu_{\rm pre}^{\rm ss}$ is obtained from an empirical formulation of saddle-to-scission transit time, given by Eq. (15). Consequently, the calculated $\nu_{\rm pre}^{\rm ss}$ can be uncertain to certain extent. It is, therefore, possible that discrepancy between experimental values and SM predictions of $\nu_{\rm pre}$ increases with projectile mass for the same CN. Such a trend is observed in general in Figs. 3–6 with the exception of ^{4}He + ^{188}Os, ^{206}Pb. The exception is possibly due to emission in the preequilibrium stage [110–114] which will be discussed shortly. It may also be mentioned here that a stronger dissipation in the saddle-to-scission region is expected to give a better fit to the experimental $\nu_{\rm pre}$. Such a shape-dependent dissipation has been reported earlier from phenomenological studies [22,23] and also from theoretical considerations [115].

One characteristic of statistical decay of CN is the expectation that the γ-ray multiplicity ($\langle M_x \rangle$) for a channel corresponding to the emission of x neutrons should increase with decreasing x, as was observed for ^{20}Ne + ^{150}Nd, since evaporation of fewer neutrons would leave more energy for γ-ray emission [116]. However, this was not the case for ^{12}C + ^{158}Gd, where $\langle M_x \rangle$ remained essentially constant for small x. This saturation effect observed in the γ-ray multiplicity of ^{12}C + ^{158}Gd, relative to the same of ^{20}Ne + ^{150}Nd at the same CN excitation energy (and slightly different angular momenta), was said to be a clear signature of preequilibrium emissions of neutrons [110,116–118]. The disagreement of theory and measurement for ^{4}He + ^{188}Os, ^{206}Pb may also be attributed to the emissions in the preequilibrium stage [110–114].

For systems with higher mass symmetry, neutrons ($\nu_{\rm pre}^{\rm exp}$) can also be emitted in the comparatively longer formation stage ($\nu_{\rm pre}^{\rm pre\text{-}eq} + \nu_{\rm pre}^{\rm NCNF}$) of the CN [76,119,120] and/or during neck rupture ($\nu_{\rm pre}^{\rm sc}$) [121–129] and/or from the acceleration phase of fission fragments ($\nu_{\rm pre}^{\rm acc}$) [60,130–132], which are not included in the present work. These are the most probable reasons for the mismatch in the experimental and the calculated $\nu_{\rm pre}$ for the symmetric combinations. Further, the $\nu_{\rm pre}^{\rm exp}$ were found to be higher than those extracted from fission chance distributions [64,133]. This indicates a significant post-saddle contribution in the $\nu_{\rm pre}^{\rm exp}$. It must be mentioned here that unlike scission neutrons, protons, due to their Coulomb repulsion, have less presence in the neck region [134].

ER is the clearest signature of fusion, and the particle multiplicities extracted in coincidence with ERs are not affected by the emissions from the later part, i.e., fission (saddle-to-scission dynamics). Therefore, ERs from highly asymmetric systems can serve as the benchmark for input parameters of the SM which fit the experimental data. For example, particle multiplicity data (in coincidence with ERs as well as FFs) of the asymmetric reaction ^{19}F + ^{181}Ta (Figs. 7 and 8) are reproduced quite well with the present SM calculations. This indicates that deformation effects in the saddle-to-scission region and other near-scission and post-scission contributions are not severe for this system. However, this is not the case for few other systems, e.g. ^{19}F, ^{28}Si + ^{197}Au, and the discrepancy possibly arises from the aforementioned processes. Moreover,

dynamical deformation may cause the observed deviation of the predicted particle multiplicities from the measured ones [135,136].

It had been noticed earlier that, while a standard set of parameters in an SM could reproduce the gross features of α-particle spectra from the ER channel, they failed in the fission channel [137]. A reduction in the emission barrier was necessary for a satisfactory reproduction of the latter. This was attributed to the large deformation of the fissioning nuclei with respect to the ER channel [109,137,138]. With increasing deformation, the binding energies of the charged particles (proton, α particles, etc.) increase whereas the effective emission barrier heights decrease. While the former lowers the emission rate, the latter enhances it [139,140]. Altogether, accounting for the effect of deformation energy, particle transmission coefficients, and particle binding energies on the emission rates leads to the suppression of the $\pi_{\rm pre}$ and $\alpha_{\rm pre}$ compared to $\nu_{\rm pre}$ [141]. Analysis of the kinetic energy spectra of the emitted light charged particles and/or an estimation of the SM branching ratios by analyzing measured $\nu_{\rm ER}$ can shed light on the origin of the overestimation of the calculated multiplicities of the symmetric reactions by the SM [10,142,143]. Aleshin [144] presented a semiclassical description for light particle emission from a composite system with a time-dependent shape. A satisfactory description of the charged particle multiplicities was achieved by taking the mean value of the particle separation energies of the two nuclei making the composite system rather than that of the mononucleus (which overestimated multiplicities) while calculating the decay widths. These aspects need further investigation.

IV. CONCLUSION

We have carried out a systematic analysis of available $\sigma_{\rm ER}$, $\sigma_{\rm fiss}$, $\nu_{\rm pre}$, $\pi_{\rm pre}$, $\alpha_{\rm pre}$ (also $\nu_{\rm ER}$, $\pi_{\rm ER}$, and $\alpha_{\rm ER}$) data covering $A_{\rm CN} = 158$–248. The shell effect in LD and shell correction in $B_{\rm f}$, effect of $K_{\rm or}$, CELD, and dissipation in fission have been considered in the SM. Parameters of the model have not been tuned to reproduce observables from specific reaction(s) except for β, the strength of the reduced dissipation coefficient, which has been treated as the only adjustable parameter in the calculation. The model is able to reproduce $\sigma_{\rm ER}$ and $\sigma_{\rm fiss}$ simultaneously for all the reactions considered in this work. Experimental $\nu_{\rm pre}$ are underestimated by the calculation in some cases. An increasingly higher strength of β (2–4×10^{21} s^{-1}) is required to reproduce the data with increasing $A_{\rm CN}$. Experimental proton and α-particle multiplicities, measured in coincidence with both ERs and FFs, are in qualitative agreement with model predictions. The present investigation thus mitigates the existing inconsistencies in modeling statistical decay of the fissile CN to a large extent. Contradictory requirements of fission enhancement—obtained by scaling down the fission barrier to reproduce $\sigma_{\rm ER}$ or $\sigma_{\rm fiss}$ and fission suppression realized by introducing dissipation in the fission channel to reproduce $\nu_{\rm pre}$, for similar reactions—are no longer called for. There are scopes for further refinement of the model, particularly in the domains of dynamical effects in the post-saddle and near-scission regions for neutrons and deformation effects on the charged particle emission widths in the post-saddle region, as is evident from the mismatch between measured and calculated light particle multiplicities in a few cases.

ACKNOWLEDGMENTS

T.B. acknowledges IUAC, New Delhi, for financial support in the form of a fellowship (IUAC/FS-1027/5876). S.P. acknowledges the kind hospitality provided by IUAC through a Visiting Associateship during the course of this work.

[1] N. Bohr, Nature (London) **137**, 344 (1936).
[2] T. Banerjee, S. Nath, and S. Pal, Phys. Lett. B **776**, 163 (2018).
[3] C. Schmitt, K. Mazurek, and P. N. Nadtochy, Phys. Lett. B **737**, 289 (2014).
[4] H. Delagrange, A. Fleury, and J. M. Alexander, Phys. Rev. C **16**, 706 (1977).
[5] F. Videbæk, R. B. Goldstein, L. Grodzins, S. G. Steadman, T. A. Belote, and J. D. Garrett, Phys. Rev. C **15**, 954 (1997).
[6] D. Ward, R. J. Charity, D. J. Hinde, J. R. Leigh, and J. O. Newton, Nucl. Phys. A **403**, 189 (1983).
[7] J. P. Lestone, Phys. Rev. Lett. **70**, 2245 (1993).
[8] B. J. Fineman, K.-T. Brinkmann, A. L. Caraley, N. Gan, R. L. McGrath, and J. Velkovska, Phys. Rev. C **50**, 1991 (1994).
[9] R. J. Charity, Phys. Rev. C **82**, 014610 (2010).
[10] A. Di Nitto, E. Vardaci, A. Brondi, G. La Rana, R. Moro, P. N. Nadtochy, M. Trotta, A. Ordine, A. Boiano, M. Cinausero *et al.*, Eur. Phys. J. A **47**, 83 (2011).
[11] D. Mancusi, R. J. Charity, and J. Cugnon, Phys. Rev. C **82**, 044610 (2010).
[12] S. G. McCalla and J. P. Lestone, Phys. Rev. Lett. **101**, 032702 (2008).
[13] J. P. Lestone and S. G. McCalla, Phys. Rev. C **79**, 044611 (2009).
[14] K.-T. Brinkmann, A. L. Caraley, B. J. Fineman, N. Gan, J. Velkovska, and R. L. McGrath, Phys. Rev. C **50**, 309 (1994).
[15] R. N. Sagaidak and A. N. Andreyev, Phys. Rev. C **79**, 054613 (2009).
[16] V. Singh, B. R. Behera, M. Kaur, A. Kumar, K. P. Singh, N. Madhavan, S. Nath, J. Gehlot, G. Mohanto, A. Jhingan *et al.*, Phys. Rev. C **89**, 024609 (2014).
[17] D. J. Hinde, R. J. Charity, G. S. Foote, J. R. Leigh, J. O. Newton, S. Ogaza, and A. Chattejee, Nucl. Phys. A **452**, 550 (1986).
[18] J. O. Newton, D. J. Hinde, R. J. Charity, J. R. Leigh, J. J. M. Bokhorst, A. Chatterjee, G. S. Foote, and S. Ogaza, Nucl. Phys. A **483**, 126 (1988).
[19] E. Vardaci, A. Di Nitto, A. Brondi, G. La Rana, R. Moro, P. N. Nadotchy, M. Trotta, A. Ordine, A. Boiano, M. Cinausero *et al.*, Eur. Phys. J. A **43**, 127 (2010).
[20] D. Hilscher and H. Rossner, Ann. Phys. Fr. **17**, 471 (1992).
[21] P. Paul and M. Thoennessen, Annu. Rev. Nucl. Part. Sci. **44**, 65 (1994).

[22] I. Diószegi, N. P. Shaw, I. Mazumdar, A. Hatzikoutelis, and P. Paul, Phys. Rev. C **61**, 024613 (2000).

[23] P. Fröbrich and I. I. Gontchar, Phys. Rep. **292**, 131 (1998).

[24] N. P. Shaw, I. Diószegi, I. Mazumdar, A. Buda, C. R. Morton, J. Velkovska, J. R. Beene, D. W. Stracener, R. L. Varner, M. Thoennessen, and P. Paul, Phys. Rev. C **61**, 044612 (2000).

[25] P. V. Laveen, E. Prasad, N. Madhavan, S. Pal, J. Sadhukhan, S. Nath, J. Gehlot, A. Jhingan, K. M. Varier, R. G. Thomas, A. M. Vinodkumar, A. Shamlath, T. Varughese, P. Sugathan, B. R. S. Babu, S. Appannababu, K. S. Golda, B. R. Behera, V. Singh, R. Sandal, A. Saxena, B. V. John, and S. Kailas, J. Phys. G: Nucl. Part. Phys. **42**, 095105 (2015).

[26] G. Mohanto, N. Madhavan, S. Nath, J. Sadhukhan, J. Gehlot, I. Mazumdar, M. B. Naik, E. Prasad, I. Mukul, T. Varughese, A. Jhingan, R. K. Bhowmik, A. K. Sinha, D. A. Gothe, P. B. Chavan, S. Pal, V. S. Ramamurthy, and A. Roy, Nucl. Phys. A **890-891**, 62 (2012).

[27] K. Ramachandran, A. Chatterjee, A. Navin, K. Mahata, A. Shrivastava, V. Tripathi, S. Kailas, V. Nanal, R. G. Pillay, A. Saxena, R. G. Thomas, S. Kumar, and P. K. Sahu, Phys. Rev. C **73**, 064609 (2006).

[28] T. Banerjee, S. Nath, A. Jhingan, N. Saneesh, M. Kumar, A. Yadav, G. Kaur, R. Dubey, M. Shareef, P. V. Laveen, A. Shamlath, Md. Moin Shaikh, S. Biswas, J. Gehlot, K. S. Golda, P. Sugathan, and S. Pal, Phys. Rev. C **96**, 014618 (2017).

[29] T. Banerjee, S. Nath, and S. Pal, Phys. Rev. C **91**, 034619 (2015).

[30] R. V. F. Janssens, R. Holzmann, W. Henning, T. L. Khoo, K. T. Lesko, G. S. F. Stephans, D. C. Radford, A. M. Van Den Berg, Phys. Lett. B **181**, 16 (1986).

[31] F. L. H. Wolfs, R. V. F. Janssens, R. Holzmann, T. L. Khoo, W. C. Ma, and S. J. Sanders, Phys. Rev. C **39**, 865 (1989).

[32] A. M. Zebelman and J. M. Miller, Phys. Rev. Lett. **30**, 27 (1973).

[33] A. Gavron, J. R. Beene, B. Cheynis, R. L. Ferguson, F. E. Obenshain, F. Plasil, G. R. Young, G. A. Petitt, M. Jääskeläinen, D. G. Sarantites, and C. F. Maguire, Phys. Rev. Lett. **47**, 1255 (1981); **48**, 835(E) (1982).

[34] J. R. Leigh, M. Dasgupta, D. J. Hinde, J. C. Mein, C. R. Morton, R. C. Lemmon, J. P. Lestone, J. O. Newton, H. Timmers, J. X. Wei, and N. Rowley, Phys. Rev. C **52**, 3151 (1995).

[35] D. J. Hinde, H. Ogata, M. Tanaka, T. Shimoda, N. Takahashi, A. Shinohara, S. Wakamatsu, K. Katori, and H. Okamura, Phys. Rev. C **37**, 2923(R) (1988).

[36] D. J. Hinde, D. Hilscher, H. Rossner, B. Gebauer, M. Lehmann, and M. Wilpert, Phys. Rev. C **45**, 1229 (1992).

[37] D. G. Sarantites, J. H. Barker, M. L. Halbert, D. C. Hensley, R. A. Dayras, E. Eichler, N. R. Johnson, and S. A. Gronemeyer, Phys. Rev. C **14**, 2138 (1976).

[38] A. M. Zebelman, L. Kowalski, J. Miller, K. Beg, Y. Eyal, G. Jaffe, A. Kandil, and D. Logan, Phys. Rev. C **10**, 200 (1974).

[39] M. L. Halbert, R. A. Dayras, R. L. Ferguson, F. Plasil, and D. G. Sarantites, Phys. Rev. C **17**, 155 (1978).

[40] A. Navin, V. Tripathi, Y. Blumenfeld, V. Nanal, C. Simenel, J. M. Casandjian, G. de France, R. Raabe, D. Bazin, A. Chatterjee, M. Dasgupta, S. Kailas, R. C. Lemmon, K. Mahata, R. G. Pillay, E. C. Pollacco, K. Ramachandran, M. Rejmund, A. Shrivastava, J. L. Sida, and E. Tryggestad, Phys. Rev. C **70**, 044601 (2004).

[41] A. V. Ignatyuk, M. G. Itkis, V. N. Okolovich, G. N. Smirenkin and A. S. Tishin, Yad. Fiz. **21**(6), 1185 (1975) [Sov. J. Nucl. Phys. **21**, 612 (1976)].

[42] R. P. Schmitt, T. Botting, G. G. Chubarian, K. L. Wolf, B. J. Hurst, H. Jabs, M. Hamelin, A. Bacak, Yu. Ts. Oganessian, M. G. Itkis, E. M. Kozulin *et al.*, Phys. Atom. Nucl. **66**, 1163 (2003).

[43] T. Rajbongshi, K. Kalita, S. Nath, J. Gehlot, Tathagata Banerjee, Ish Mukul, R. Dubey, N. Madhavan, C. J. Lin, A. Shamlath, P. V. Laveen, M. Shareef, N. Kumar, P. Jisha, and P. Sharma, Phys. Rev. C **93**, 054622 (2016).

[44] D. Singh, Unnati, P. P. Singh, A. Yadav, M. K. Sharma, B. P. Singh, K. S. Golda, R. Kumar, A. K. Sinha, and R. Prasad, Phys. Rev. C **80**, 014601 (2009).

[45] M. Ogihara, H. Fujiwara, S. C. Jeong, W. Galster, S. M. Lee, Y. Nagashima, T. Mikumo, H. Ikezoe, K. Ideno, Y. Sugiyama, and Y. Tomita, Z. Phys. A **335**, 203 (1990).

[46] B. R. Behera, S. Roy, P. Basu, M. K. Sharan, S. Jena, M. Satpathy, M. L. Chatterjee, and S. K. Datta, Pramana **57**, 199 (2001).

[47] H. Singh, A. Kumar, B. R. Behera, I. M. Govil, K. S. Golda, P. Kumar, A. Jhingan, R. P. Singh, P. Sugathan, M. B. Chatterjee, S. K. Datta, Ranjeet, S. Pal, and G. Viesti, Phys. Rev. C **76**, 044610 (2007).

[48] P. D. Shidling, N. M. Badiger, S. Nath, R. Kumar, A. Jhingan, R. P. Singh, P. Sugathan, S. Muralithar, N. Madhavan, A. K. Sinha, S. Pal *et al.*, Phys. Rev. C **74**, 064603 (2006).

[49] J. R. Leigh, J. J. M. Bokhorst, D. J. Hinde, and J. O. Newton, J. Phys. G: Nucl. Phys. **14**, L55 (1988).

[50] C. E. Bemis, Jr., T. C. Awes, J. R. Beene, R. L. Ferguson, H. J. Kim, F. K. McGowan, F. E. Obenshain, F. Plasil, P. Jacobs, Z. Frankel, U. Smilansky, and I. Tserruya, ORNL physics division progress report 6326, 1986 (unpublished).

[51] J. S. Forster, I. V. Mitchell, J. U. Andersen, A. S. Jensen, E. Laegsgaard, W. M. Gibson, and K. Reichelt, Nucl. Phys. A **464**, 497 (1987).

[52] R. J. Charity, J. R. Leigh, J. J. M. Bokhorst, A. Chatterjee, G. S. Foote, D. J. Hinde, J. O. Newton, S. Ogaza, and D. Ward, Nucl. Phys. A **457**, 441 (1986).

[53] D. J. Hinde, J. R. Leigh, J. O. Newton, W. Galster, and S. Sie, Nucl. Phys. A **385**, 109 (1982).

[54] G. Mohanto, N. Madhavan, S. Nath, J. Gehlot, I. Mukul, A. Jhingan, T. Varughese, A. Roy, R. K. Bhowmik, I. Mazumdar, D. A. Gothe, P. B. Chavan, J. Sadhukhan, S. Pal, M. Kaur, V. Singh, A. K. Sinha, and V. S. Ramamurthy, Phys. Rev. C **88**, 034606 (2013).

[55] Y. Le Beyec and M. Lefort, Nucl. Phys. A **99**, 131 (1967).

[56] E. Gadioli, I. Iori, N. Molho, and L. Zetta, Lett. Nuovo Cimento **2**, 904 (1969).

[57] A. Khodai-Joopari, Ph.D. Thesis, Report UCRL-16489, Berkeley (1966).

[58] A. V. Ignatyuk, M. G. Itkis, I. A. Kamenev, S. I. Mulgin, V. N. Okolovich, and G. N. Smirenkin, Yad. Fiz. **40**, 625 (1984) [Sov. J. Nucl. Phys. **40**, 400 (1984)].

[59] O. E. Shigaev, V. S. Bychenkov, M. F. Lomanov, A. I. Obukhov, N. A. Perfilov, G. G. Shimchuk, and R. M. Yakovlev, and V. G. Khlopin, Radium Institute, St. Petersburg, Preprint RI-17 (1973); Yadernaya Fizika **17**, 947 (1973) [Sov. J. Nucl. Phys. **17**, 496 (1974)].

[60] E. Cheifetz, Z. Fraenkel, J. Galin, M. Lefort, J. Péter, and X. Tarrago, Phys. Rev. C **2**, 256 (1970).

[61] P. R. Bimbot, H. Zaffrezic, Y. Le Beyec, M. Lefort, and A. Vigny-Simon, Le Journal de Physique **30**, 513 (1969).

[62] A. Shrivastava, S. Kailas, A. Chatterjee, A. Navin, A. M. Samant, P. Singh, S. Santra, K. Mahata, B. S. Tomar, and G. Pollarolo, Phys. Rev. C **63**, 054602 (2001).

[63] J. van der Plicht, H. C. Britt, M. M. Fowler, Z. Fraenkel, A. Gavron, J. B. Wilhelmy, F. Plasil, T. C. Awes, and G. R. Young, Phys. Rev. C **28**, 2022 (1983).

[64] K. S. Golda, A. Saxena, V. K. Mittal, K. Mahata, P. Sugathan, A. Jhingan, V. Singh, R. Sandal, S. Goyal, J. Gehlot, A. Dhal, B. R. Behera, R. K. Bhowmik, and S. Kailas, Nucl. Phys. A **913**, 157 (2013).

[65] D. J. Hinde, A. C. Berriman, R. D. Butt, M. Dasgupta, I. I. Gontchar, C. R. Morton, A. Mukherjee, and J. O. Newton, J. Nucl. Radiochem. Sci. **3**, 31 (2002).

[66] R. N. Sagaidak, G. N. Kniajeva, I. M. Itkis, M. G. Itkis, N. A. Kondratiev, E. M. Kozulin, I. V. Pokrovsky, A. I. Svirikhin, V. M. Voskressensky, A. V. Yeremin *et al.*, Phys. Rev. C **68**, 014603 (2003).

[67] H. Singh, K. S. Golda, S. Pal, Ranjeet, R. Sandal, B. R. Behera, G. Singh, A. Jhingan, R. P. Singh, P. Sugathan, M. B. Chatterjee, S. K. Datta, A. Kumar, G. Viesti, and I. M. Govil, Phys. Rev. C **78**, 024609 (2008).

[68] G. L. Bate and J. R. Huizenga, Phys. Rev. **133**, B1471 (1964).

[69] A. T. Kandil, J. Inorg. Nucl. Chem. **38**, 37 (1976).

[70] M. Strecker, R. Wien, P. Plischke, and W. Scobel, Phys. Rev. C **41**, 2172 (1990).

[71] V. A. Rubchenya, W. H. Trzaska, D. N. Vakhtin, J. Äystö, P. Dendooven, S. Hankonen, A. Jokinen, Z. Radivojevich, J. C. Wang, I. D. Alkhazov, A. V. Evsenin *et al.*, Nucl. Instrum. Methods A **463**, 653 (2001).

[72] H. Freiesleben, G. T. Rizzo, and J. R. Huizenga, Phys. Rev. C **12**, 42 (1975).

[73] D. J. Hinde, H. Ogata, M. Tanaka, T. Shimoda, N. Takahashi, A. Shinohara, S. Wakamatsu, K. Katori, and H. Okamura, Phys. Rev. C **39**, 2268 (1989).

[74] Z. Liu, H. Zhang, J. Xu, Y. Qiao, X. Qian, and C. Lin, Phys. Rev. C **54**, 761 (1996).

[75] S. Kailas, D. M. Nadkarni, A. Chatterjee, A. Saxena, S. S. Kapoor, R. Vandenbosch, J. P. Lestone, J. F. Liang, D. J. Prindle, A. A. Sonzogni, and J. D. Bierman, Phys. Rev. C **59**, 2580 (1999).

[76] A. Saxena, A. Chatterjee, R. K. Choudhury, S. S. Kapoor, and D. M. Nadkarni, Phys. Rev. C **49**, 932 (1994).

[77] B. B. Back, R. R. Betts, J. E. Gindler, B. D. Wilkins, S. Saini, M. B. Tsang, C. K. Gelbke, W. G. Lynch, M. A. McMahan, and P. A. Baisden, Phys. Rev. C **32**, 195 (1985).

[78] R. Vandenbosch, T. Murakami, C.-C. Sahm, D. D. Leach, A. Ray, and M. J. Murphy, Phys. Rev. Lett. **56**, 1234 (1986).

[79] D. M. Nadkarni, A. Saxena, D. C. Biswas, R. K. Choudhury, S. S. Kapoor, N. Majumdar, and P. Bhattacharya, Phys. Rev. C **59**, 580(R) (1999).

[80] P. N. Nadotchy, A. Brondi, A. Di Nitto, G. La Rana, R. Moro, E. Vardaci, A. Ordine, A. Boiano, M. Cinausero, G. Prete, V. Rizzi, N. Gelli, and F. Lucarelli, EPJ Web Conf. **2**, 08003 (2010).

[81] H. Ikezoe, Y. Nagame, I. Nishinaka, Y. Sugiyama, Y. Tomita, K. Ideno, S. Hamada, N. Shikazono, A. Iwamoto, and T. Ohtsuki, Phys. Rev. C **49**, 968 (1994).

[82] H. Ikezoe, N. Shikazono, Y. Nagame, Y. Sugiyama, Y. Tomita, K. Ideno, I. Nishinaka, B. J. Qi, H. J. Kim, A. Iwamoto, and T. Ohtsuki, Phys. Rev. C **46**, 1922 (1992).

[83] A. L. Caraley, B. P. Henry, J. P. Lestone, and R. Vandenbosch, Phys. Rev. C **62**, 054612 (2000).

[84] D. Fabris, E. Fioretto, G. Viesti, M. Cinausero, N. Gelli, K. Hagel, F. Lucarelli, J. B. Natowitz, G. Nebbia, G. Prete, and R. Wada, Phys. Rev. C **50**, R1261 (1994).

[85] C. R. Morton, D. J. Hinde, J. R. Leigh, J. P. Lestone, M. Dasgupta, J. C. Mein, J. O. Newton, and H. Timmers, Phys. Rev. C **52**, 243 (1995).

[86] N. Bohr and J. A. Wheeler, Phys. Rev. **56**, 426 (1939).

[87] K. Hagino, N. Rowley, and A. T. Kruppa, Comput. Phys. Commun. **123**, 143 (1999).

[88] A. J. Sierk, Phys. Rev. C **33**, 2039 (1986).

[89] W. D. Myers and W. J. Swiatecki, Nucl. Phys. **81**, 1 (1966).

[90] A. V. Ignatyuk, M. G. Itkis, V. N. Okolovich, G. M. Smirenkin, and A. Tishin, Yad. Fiz. **21**, 485 (1975) [Sov. J. Nucl. Phys. **21**, 255 (1975)].

[91] W. Reisdorf, Z. Phys. A **300**, 227 (1981).

[92] S. Bjørnholm, A. Bohr, and B. R. Mottelson, in *Proceedings of the International Conference on the Physics and Chemistry of Fission*, Rochester, 1973 (IAEA, Vienna, 1974), Vol. 1, p. 367.

[93] A. V. Ignatyuk, G. N. Smirenkin, M. G. Itkis, S. I. Mul'gin, and V. N. Okolovich, Fiz. Elem. Chastits At. Yadra **16**, 709 (1985) [Sov. J. Part. Nucl. **16**, 307 (1985)].

[94] V. I. Zagrebaev, Y. Aritomo, M. G. Itkis, Y. T. Oganessian, and M. Ohta, Phys. Rev. C **65**, 014607 (2001).

[95] A. R. Junghans, M. de Jong, H.-G. Clerc, A. V. Ignatyuk, G. A. Kudyaev, and K.-H. Schmidt, Nucl. Phys. A **629**, 635 (1998).

[96] M. Ohta, in *Proceedings on Fusion Dynamics at the Extremes*, Dubna, 2000, edited by Yu. Ts. Oganessian and V. I. Zagrebaev (World Scientific, Singapore, 2001), p. 110.

[97] K. Banerjee, P. Roy, D. Pandit, J. Sadhukhan, S. Bhattacharya, C. Bhattacharya, G. Mukherjee, T. K. Ghosh, S. Kundu, A. Sen, T. K. Rana, S. Manna, R. Pandey, T. Roy, A. Dhal, Md. A. Asgar, and S. Mukhopadhyay, Phys. Lett. B **772**, 105 (2017).

[98] D. Pandit, S. Bhattacharya, D. Mondal, P. Roy, K. Banerjee, S. Mukhopadhyay, S. Pal, A. De, B. Dey, and S. R. Banerjee, Phys. Rev. C **97**, 041301(R) (2018).

[99] J. P. Lestone, Phys. Rev. C **59**, 1540 (1999).

[100] H. A. Kramers, Physica **7**, 284 (1940).

[101] J. Sadhukhan and S. Pal, Phys. Rev. C **78**, 011603(R) (2008); **79**, 019901(E) (2009).

[102] J. Blocki, Y. Boneh, J. R. Nix, J. Randrup, M. Robel, A. J. Sierk, and W. J. Swiatecki, Ann. Phys. **113**, 330 (1986).

[103] H. Hofmann, Phys. Rep. **284**, 137 (1997).

[104] T. Mukhopadhyay and S. Pal, Phys. Rev. C **56**, 296 (1997).

[105] P. Grangé, L. Jun-Qing, and H. A. Weidenmüller, Phys. Rev. C **27**, 2063 (1983).

[106] K. H. Bhatt, P. Grangé, and B. Hiller, Phys. Rev. C **33**, 954 (1986).

[107] H. Hofmann and J. R. Nix, Phys. Lett. B **122**, 117 (1983).

[108] G. Chaudhuri and S. Pal, Phys. Rev. C **65**, 054612 (2002).

[109] J. P. Lestone, J. R. Leigh, J. O. Newton, D. J. Hinde, J. X. Wei, J. X. Chen, S. Elfstrom, and M. Zielinska-Pfabe, Nucl. Phys. A **559**, 277 (1993).

[110] D. G. Sarantites, L. Westerberg, R. A. Dayras, M. L. Halbert, D. C. Hensley, and J. H. Barker, Phys. Rev. C **17**, 601 (1978).

[111] N. L. Singh, S. Agarwal and J. Rama Rao, J. Phys. G: Nucl. Part. Phys. **18**, 927 (1992).

[112] N. Chakravarty, P. K. Sarkar, and S. Ghosh, Phys. Rev. C **45**, 1171 (1992).
[113] K. Knoche, L. Lüdemann, W. Scobel, B. Gebauer, D. Hilscher, D. Polster, and H. Rossner, Phys. Rev. C **51**, 1908 (1995).
[114] B. P. Singh, M. K. Sharma, M. M. Musthafa, H. D. Bhardwaj, and R. Prasad, Nucl. Instrum. Methods A **562**, 717 (2006).
[115] S. Pal and T. Mukhopadhyay, Phys. Rev. C **57**, 210 (1998).
[116] D. G. Sarantites, L. Westerberg, M. L. Halbert, R. A. Dayras, D. C. Hensley, and J. H. Barker, Phys. Rev. C **18**, 774 (1978).
[117] M. Blann, Nucl. Phys. A **235**, 211 (1974).
[118] L. Westerberg, D. G. Sarantites, D. C. Hensley, R. A. Dayras, M. L. Halbert, and J. H. Barker, Phys. Rev. C **18**, 796 (1978).
[119] S. E. Vigdor, H. J. Karwowski, W. W. Jacobs, S. Kailas, P. P. Singh, F. Soga, and T. G. Throwe, Phys. Rev. C **26**, 1035 (1982).
[120] J. Cabrera, Th. Keutgen, Y. El Masri, Ch. Dufauquez, V. Roberfroid, I. Tilquin, J. Van Mol, R. Regimbart, R. J. Charity, J. B. Natowitz, K. Hagel, R. Wada, and D. J. Hinde, Phys. Rev. C **68**, 034613 (2003).
[121] H. R. Bowman, S. G. Thompson, J. C. D. Milton, and W. J. Swiatecki, Phys. Rev. **126**, 2120 (1962).
[122] W. D. Loveland, A. W. Fairhall, and I. Halpern, Phys. Rev. **163**, 1315 (1967).
[123] I. Halpern, Annu. Rev. Nucl. Part. Sci **21**, 245 (1971).
[124] C. B. Franklyn, C. Hofmeyer, and D. W. Mingay, Phys. Lett. **78B**, 564 (1978).
[125] U. Brosa and S. Grossmann, Z. Phys. A **310**, 177 (1983).
[126] J. K. Hwang, A. V. Ramayya, J. H. Hamilton, W. Greiner, J. D. Cole, G. M. Ter-Akopian, Yu. Ts. Oganessian, and A. V. Daniel (GANDS95 Collaboration), Phys. Rev. C **60**, 044616 (1999).
[127] N. V. Kornilov, F.-J. Hambsch, and A. S. Vorobyev, Nucl. Phys. A **789**, 55 (2007).
[128] N. Carjan and M. Rizea, Phys. Rev. C **82**, 014617 (2010).
[129] R. Capote, Chen Y.-J., F.-J. Hambsch, N. V. Kornilov, J. P. Lestone, O. Litaize, B. Morillon, D. Neudecker, S. Oberstedt, and T. Ohsawa, Nucl. Data Sheets **131**, 1 (2016).
[130] V. P. Eismont, Sov. J. At. Energy **19**, 1000 (1965).
[131] K. Skarsvag, Phys. Scr. **7**, 160 (1973).
[132] D. J. Hinde, R. J. Charity, G. S. Foote, J. R. Leigh, J. O. Newton, S. Ogaza, and A. Chatterjee, Phys. Rev. Lett. **52**, 986 (1984).
[133] K. Mahata and S. Kailas, Phys. Rev. C **95**, 054616 (2017).
[134] N. Carjan and M. Rizea, Phys. Lett. B **747**, 178 (2015).
[135] W. Ye, Phys. Rev. C **81**, 054609 (2010).
[136] N. Kumar, S. Mohsina, J. Sadhukhan, and S. Verma, Phys. Rev. C **96**, 034614 (2017).
[137] E. Vardaci, G. La Rana, A. Brondi, R. Moro, A. Principe, D. Fabris, G. Nebbia, G. Viesti, M. Cinausero, E. Fioretto *et al.*, Eur. Phys. J. A **2**, 55 (1998).
[138] H. Ikezoe, N. Shikazono, Y. Nagame, Y. Sugiyama, Y. Tomita, K. Ideno, A. Iwamoto, and T. Ohtsuki, Phys. Rev. C **42**, 342 (1990).
[139] M. Beckerman and M. Blann, Phys. Rev. Lett. **42**, 156 (1979).
[140] M. Blann, Phys. Rev. C **21**, 1770 (1980).
[141] J. P. Lestone, J. R. Leigh, J. O. Newton, D. J. Hinde, J. X. Wei, J. X. Chen, S. Elfstrom, and D. G. Popescu, Phys. Rev. Lett. **67**, 1078 (1991).
[142] J. L. Wile, D. L. Coffing, E. T. Bauer, A. L. Michael, M. A. Doerner, S. P. Baldwin, B. M. Szabo, B. Lott, B. M. Quednau, J. Tõke, W. U. Schröder, and R. T. de Souza, Phys. Rev. C **51**, 1693 (1995).
[143] Sh. A. Kalandarov, G. G. Adamian, and N. V. Antonenko, EPJ Web Conf. **38**, 09002 (2012).
[144] V. P. Aleshin, J. Phys. G: Nucl. Part. Phys. **19**, 307 (1993).